A simple three step method for selective placement of organic groups in mesoporous silica thin films

Esteban A. Franceschini [a], Ezequiel de la Llave [b], Federico J. Williams [b], Galo J.A.A. Soler-Illia [b, c, *]

[a] Gerencia Química, Centro Atómico Constituyentes, Comisión Nacional de Energía Atómica, Av. Gral Paz 1499 (B1650KNA) San Martín, Buenos Aires, Argentina
[b] Departamento de Química Inorgánica, Analítica y Química Física and INQUIMAE-CONICET, Facultad de Ciencias Exactas y Naturales, Universidad de Buenos Aires, Ciudad Universitaria, Pabellón II, C1428EHA Buenos Aires, Argentina
[c] Instituto de Nanosistemas, Universidad Nacional de General San Martín, 25 de Mayo y Francia (1650) San Martín, Buenos Aires, Argentina

HIGHLIGHTS

- Selective functionalization of mesoporous silica thin films was achieved using a three step method.
- A volatile silane group is anchored by evaporation on the outer film surface.
- A second silane is deposited in the inner surface of the pores by post-grafting.
- Contact angle, EDS and XPS measurements show different proportions of amino groups on both surfaces.
- This method can be extended to a combination of silane chlorides and alkoxides functional groups.

GRAPHICAL ABSTRACT
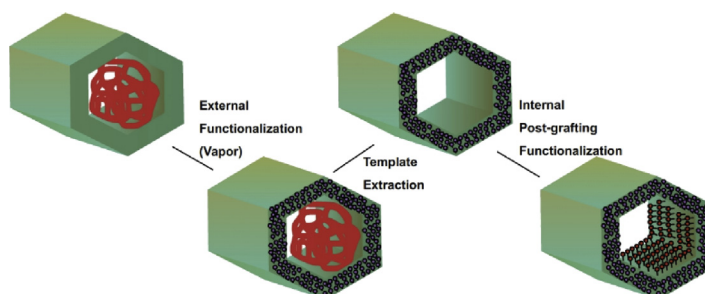
ARTICLE INFO

ABSTRACT

Selective functionalization of mesoporous silica thin films was achieved using a three step method. The first step consists in an outer surface functionalization, followed by washing off the structuring agent (second step), leaving the inner surface of the pores free to be functionalized in the third step. This reproducible method permits to anchor a volatile silane group in the outer film surface, and a second type of silane group in the inner surface of the pores. As a concept test we modified the outer surface of a mesoporous silica film with trimethylsilane ($-Si-(CH_3)_3$) groups and the inner pore surface with propylamino ($-Si-(CH_2)_3-NH_2$) groups. The obtained silica films were characterized by Environmental Ellipsometric Porosimetry (EEP), EDS, XPS, contact angle and electron microscopy. The selectively functionalized silica (SF) shows an amount of surface amino functions 4.3 times lower than the one-step functionalized (OSF) silica samples. The method presented here can be extended to a combination of silane chlorides and alkoxides as functional groups, opening up a new route toward the synthesis of multifunctional mesoporous thin films with precisely localized organic functions.

* Corresponding author. Instituto de Nanosistemas, Universidad Nacional de General San Martín, 25 de Mayo y Francia (1650) San Martín, Buenos Aires, Argentina.
E-mail addresses: galo.soler.illia@gmail.com, gsoler-illia@unsam.edu.ar (G.J.A.A. Soler-Illia).

1. Introduction

Mesoporous hybrid thin films (MHTF) with high surface area, periodically organized porosity and versatile pore surface functionalization constitute a thriving field in current materials chemistry [1–3]. In the last years, significant advances have been reported in the reproducible MHTF production and properties control, which bring up potential advanced applications in energy, sensing, prosthetics and information technology, among others. In addition, MHTF can be easily integrated in electronic or micro/nanofluidic platforms [2–4]. The incorporation of active organic groups in nanosized materials is the basic principle of the rational design of "on-demand" hybrid assemblies for multiple applications [5,6]. The physically constrained environment plays a central role in determining the molecular organization and chemical reactivity, mainly due to interfacial interactions, symmetry breaking, and confinement-induced entropy losses [7,8].

Chemical strategies to preparing organo/inorganic nanostructured materials following the concepts of soft chemistry and assembled materials have been widely reported [9–11] and include the access of grafting reagents as organo-chloro or alkoxysilanes to the internal Si–OH groups located in the pore surface of meso-ordered materials [12–14]. Liz-Marzán et al. had successfully carried out silane grafting in mesoporous particles using a solvent-free method at room temperature comprising the volatilization of (3-aminopropyl)-dimethyl-ethoxysilane (APDMES) with bubbling N_2 [15,16]. This route was preferred over solution-phase silanization, since it proved to have no effect on the adhesion of the silica particles, and improves the efficiency of silane grafting.

The processes that take place in the internal surface of a mesopore can be significantly different to the processes occurring in the external surface of the mesoporous material, which is in contact with the bulk solution. This is particularly important in the design of sophisticated nanosystems, for example gated nanoporous architectures, in which the outer groups control long-range interactions and wetting, while inner groups control molecular transport [17].

In the case of mesoporous films with highly uniform and open pore systems, a precise separation between both types of functions (e. g. hydrophobic/ion complexing, hydrophilic/hydrophobic, bioactive/drug release) is required for advanced applications in fields such as micro- and nanofluidics, separation membranes, biopore mimetic systems, controlled cell adhesion or drug delivery membranes. Mesoporous thin films present typical thicknesses in the order of 100 nm, hence diffusion is a fast process [3]. To date, very few simple and reproducible techniques have been reported that enable the separate selective grafting of two different functions on the external film and the inner pore surface [18–21]. A careful control of the reactivity must be achieved in the case of films, because if the surface function penetrates along the mesopores, the precision in the function distribution can be lost, or even pore clogging can occur. Thus, promoting a fast anchoring of a first function in the presence of the template in the first step seems to be essential. Alternatively, one can resort to multi-step processes relying on the control of wetting and capillary effects of solvents with different philicity that block the pores as a kind of "nano stoppers" [22,23].

Ruiz-Hitzky and De Juan were the first to present a route to produce mesoporous particulated silica with a selective functionalization of the internal and external surfaces of the material. In this method, the selective intra (aryl)- or extra (alkyl)- pore functionalization was carried out [18].

Control of transport and reactivity of functional groups has been used to selectively place organic functions along the mesoporous channels. Lim and Stein showed that post-grafting leads to a gradient in function incorporation, which was enriched at the pore outlets [19]. Brühwiler et al. developed techniques to follow in-situ the functionalization [24], and established the kinetics. Shephard et al. [25] developed a method to passivate the external surface of MCM-41 with small amounts of diphenyldichlorosilane. Subsequent grafting of APTMS would then lead to an exclusive amino-functionalization of the pore surface. The position of the surface-grafted amino groups was determined by high resolution TEM and following adsorption of a ruthenium cluster compound. Bein and coworkers [20,21] have developed a selective functionalization procedure with a sequential co-condensation approach via functionalized oligosilicates. Using this strategy, they achieve an outer and inner surfaces functionalization in mesoporous silica particles with spatial control of organic groups without significantly decreasing the pore accessibility. These strategies are well suited for mesoporous particles, in which the particle size, geometry and tortuosity of the pores result in relatively long diffusion times that would allow its use in, for instance, the design of drug delivery systems [26]. However, it must be recalled that incorporation of organic functions by co-condensation methods often leads to the burying of such functional groups within the mesopores walls, precluding their full exposure to the pore interior or the external surface [19,36].

As far as we know, the usual methods presented in literature adapted for powders have limitations when applied to supported thin films. Repeated exposure to high temperatures and solution media containing functional molecules such as silanes can lead to pore clogging or partial silica dissolution [18]. These effects might represent a minor loss in a powdered material, but can seriously degrade the performance of a thin coating, which presents very low masses (in the order of magnitude of mg cm^{-2}) [27–30].

In this work we propose a soft alternative method that enables the rapid and selective functionalization of mesoporous silica thin films from controlled vapor deposition of alkoxides. This method does not affect the stability of the material, and leaves the pore surface intact. In addition, this simple three-step method does not require high working temperatures nor aggressive media, allowing the functionalization with a wide variety of volatile silanes. The first step of the method consists in the functionalization of the outer surface of a mesoporous silica thin film in which the pore template has not been removed. The second step consists in washing off the template, thus leaving the inner surface of the pores free to be functionalized in a third step, with a silane different to the one used in the first step. Targeted groups for the selective functionalization were trimethylchlorosilane (TMCS), and (3-Aminopropyl)triethoxysilane (APTES). These silanes were chosen as model groups since they have large physical-chemical differences as a result of the different functional groups. These chemical differences allow to probe the location of the groups in the porous matrix by techniques such as EDS and XPS, and additionally confer to the surfaces measurable properties such as different degrees of hydrophobicity/hydrophilicity. In addition, they present marked reactivity differences, in order to optimize their positioning. The synthesized materials were characterized using superficial and bulk analysis techniques in order to evaluate the chemical functions present on the film surface, and the interior of the mesopores. The possibility of separately functionalizing the inner and outer surfaces of these materials has important consequences in relevant issues regarding mesoporous coatings, such as adhesion control, microfluidics, selective sensing, catalysis and drug delivery systems.

2. Experimental

2.1. Materials

Polyethylene glycol hexadecyl ether, denoted Brij 58® (Mw = 1,124, Aldrich), absolute ethanol (99.8%, Research S.A.), hydrochloric acid (37%, ACS reagent), Tetraethoxysilane (TEOS, 99,999%, Sigma–Aldrich), toluene anhydrous (99.8%, Sigma–Aldrich), trimethylchlorosilane (TMCS, 97%, Sigma–Aldrich), and (3-Aminopropyl)triethoxysilane (APTES, 99% Sigma–Aldrich) were used as received. High purity N_2 (Indura S.A.) was used as carrier gas for the first functionalization.

2.2. Synthesis

2.2.1. Mesoporous silica films synthesis

Mesoporous silica thin films were obtained via the combination of sol–gel and self-assembly of a surfactant template. Dip coating was performed onto silicon wafer substrates (University Wafer), which allows obtaining homogeneous and transparent mesoporous thin films with good adherence. A 2 mm s^{-1} withdrawal speed was used employing a sol containing tetraethoxysilane as the oxide precursor, ethanol, water, and HCl as catalyst (TEOS:EtOH:H_2O:HCl = 1:3:1:5 × 10^{-5}). Nonionic template Brij 58® was used as template. This experimental protocol [31] led to ~200 nm thick mesoporous silica films presenting large, easily accessible mesopores. A post-treatment was carried out to achieve the consolidation of mesoporous silica structure avoiding the degradation of the Brij 58® template [32]. Freshly synthesized silica films were kept for 24 h at room temperature under a controlled atmosphere of 50% relative humidity, followed by successive 24 h treatments at 60 °C and 130 °C. Finally, the films were calcined from 130° C to 200 °C with a heating rate of 1° C min^{-1}, and kept at this final temperature for 2 h, in order to consolidate the inorganic network.

2.2.2. Mesoporous silica functionalization

Two kinds of samples were synthesized in order to prove the selective functionalization of the material, as described below and schematized in Fig. 1. Full functionalization with APTES over the pores and upper film surface was performed using a one step functionalization (OSF) post-grafting technique, while a selective functionalization (SF) procedure was developed in consecutive steps.

In the case of the one step functionalization (OSF) post-grafting, APTES functionalization was performed over the entire surface. Once the silica film was consolidated at 200 °C, the surfactant was removed with HCl/ethanol solution, as described above. Then, the films were placed in a 2 × 10^{-3} M APTES solution in toluene, keeping the system at 60 °C for 24 h. Once this period, the samples were washed and kept in ethanol for 24 h.

The selective functionalization process (i.e., SF samples) was performed in successive steps. The first functionalization of the external surface was carried out by exposing the films to TMCS vapor (step 1). Silica film samples treated at 200 °C for consolidation (i.e., still containing the surfactant) were placed in a semi-closed vessel. A two-way plastic container was loaded with 0.1 g of the functionalizing precursor, and connected to the vessel, and to a syringe injecting 50 ml min^{-1} of N_2 as carrier gas. This system was maintained in flow until depletion of the TMCS (about 30 min). Once completed, the samples were washed several times with dry ethanol. Subsequently, the film was introduced into a solution of HCl in ethanol (0.1 M) for 24 h to remove the surfactant, and copious washes were performed with ethanol to remove Brij 58®
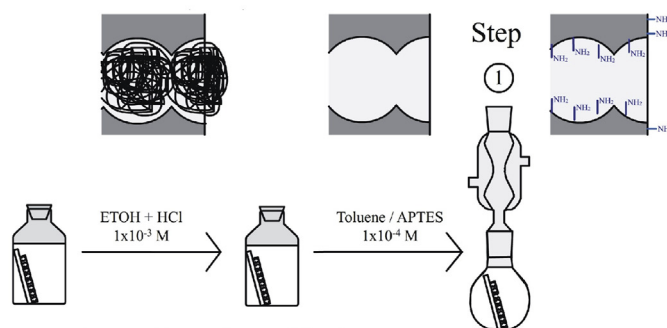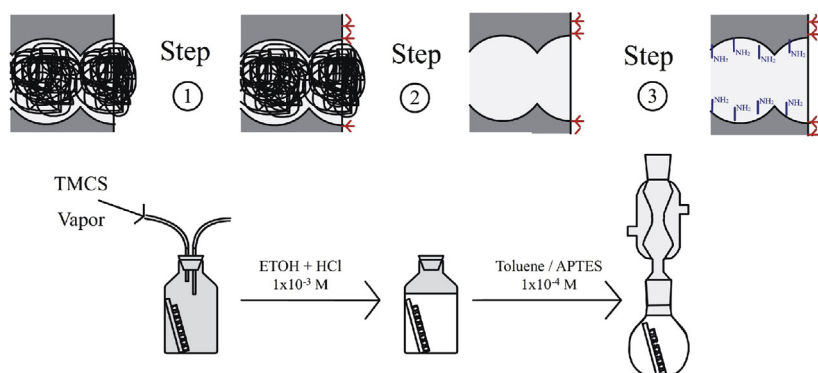

Fig. 1. Scheme of the OSF silica and SF silica synthesis.

traces that may remain (step 2). Finally, the second functionalization with amino group (internal) was carried out using a 2×10^{-3} M APTES solution in toluene, keeping the system at 60 °C for 24 h (step 3). After this period, the films were washed and kept in ethanol for 24 h.

2.3. Characterization

Electron microscopy was performed at the Centro de Microscopías Avanzadas, Facultad de Ciencias Exactas y Naturales, UBA. Field Emission Scanning Electron micrographs were obtained using a Supra 40 (Zeiss Company) FE-SEM operating at a low voltage of 3 kV, equipped with an Oxford EDX accessory. EDS analysis was performed on films samples scratched off the substrate, in order to avoid the substrate signals. TEM was performed in a Phillips EM 301 TEM operated at 60 kV.

Ellipsometric measurements were performed in a SOPRA GES5A spectrometric ellipsometer with the use of a microspot optical configuration at an incidence angle of 74°. Before performing the measurements, the films were washed with ethanol and dried at 130 °C. The obtained data was analyzed by Winelli II software; the fitting procedures allowed the accurate determination of the refractive index function $n(\lambda)$ and the film thickness. Water adsorption−desorption isotherms were obtained by Environmental Ellipsometric Porosity (EEP), performing ellipsometry measurements under controlled relative humidity (RH); film accessible pore volume and pore size distribution were obtained according to the method proposed by Boissiere et al. [33].

X-ray photoelectron spectroscopy (XPS) measurements were performed under UHV conditions (base pressure $<5 \cdot 10^{-10}$ mbar) with a SPECS UHV spectrometer system equipped with 150 mm mean radius hemispherical electron energy analyzer and a nine channeltron detector. Spectra were acquired at a constant pass energy of 20 eV using a MgKα (1253.6 eV) source operated at 12.5 kV and 20 mA and a detection angle of 30° with respect to the sample normal. Previously to the measurements, a calibration of the energy scale was performed using sputter-cleaned gold [Au $4f_{7/2}$; binding energy (BE) = 84.00 eV] and clean copper (Cu $2p_{3/2}$; BE = 933.67 eV) samples.

Static contact angle measurements of the as prepared surfaces were measured at room temperature with a Ramé-Hart 350 goniometer. All the contact angles were determined by averaging values measured at three different points on each surface. The pH of the used milli Q water was ~5.

3. Results and discussion

Obtained films present even thickness and well-defined ordered mesoporosity. Fig. 2 shows a scanning electron image of a synthesized silica film after template extraction. The samples present mesopores of ~4 nm in diameter (measured directly from the FE-SEM and TEM images), which is the expected value for this type of materials [34]. SAXS patterns (Fig. 2a, inset) can be indexed in an *Im3m* symmetry, which is typical for this type of surfactant. The films were measured after the different functionalization processes and the extraction of structuring agent. No relevant differences were appreciated in the mesoporous structure order after processing, which evidences no alteration of the mesostructure of the film under these conditions.

The contact angle of the surface was measured in order to characterize physicochemical changes (hydrophobicity/hydrophilicity) of the surfaces functionalized with various groups. Contact angle is a very sensitive proof for surface functionalization, and the marked differences in hydrophilicity of TMCS (in the SF sample) and APTES (in the OSF sample) should lead to
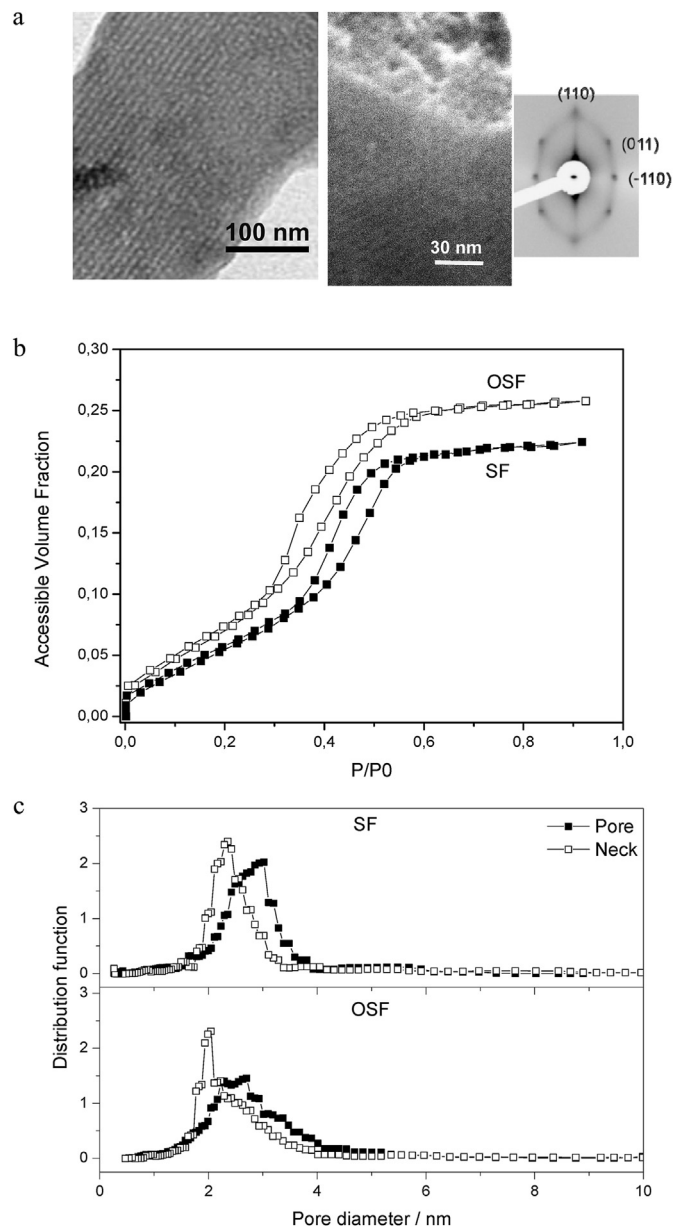

Fig. 2. a) From left to right: TEM and SEM micrographs, and typical SAXS pattern obtained in transmission at 3° of the Brij 58®-templated mesoporous silica thin films; the signals corresponding to the in-plane reflections of an Im3m cubic mesophase are indicated in the SAXS pattern. **b)** EEP of OSF (open squares) and SF (filled squares) samples. **c)** pore and neck diameter distributions.

distinctive responses, indicative of the presence of such groups at the outer surface. While TMCS is highly hydrophobic, the APTES dangling groups are hydrophilic or hydrophobic depending on the pH, due to the protonation of the amino groups and the surfaces [35]. Additionally, the study of the contact angles is essential for a proper adjustment of the results of EEP information [33].

Table 1 shows the contact angle measurements for three samples: a non-functionalized silica (NFS), and the OSF and SF templated silica thin films. The results for the non-functionalized silica are similar to those found in literature for this type of material (~30°). The surface Si−OH groups are deprotonated at pH = 5, by which the surface is charged and hydrophilic, so that the contact angle with water is relatively low [36].
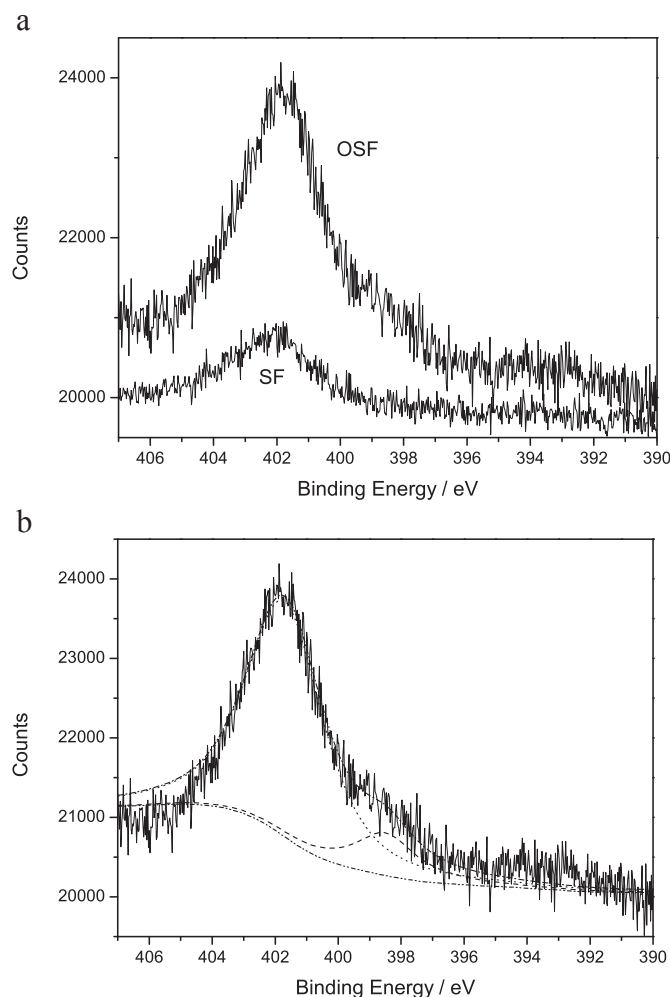
a

b

Fig. 3. **a)** N 1s XP spectra of OSF and SF. **b)** N 1s XP spectra of OSF (solid line) deconvoluted into components corresponding to −NH$_2$ (dashed line) and −NH$_3^+$ (dotted line) groups, along with the background and sum lines.

The contact angle values of the OSF sample (~70°) are higher than those obtained for the NF silica, and similar to those obtained in the literature [36,37]. This partial loss of the hydrophilic character of the surface is an expected result for APTES functionalized mesoporous silica. The material with the OSF is expected to present partially dissociated −NH$_2$ groups on its outer surface at pH = 5, due to the interplay of acid-base behaviors of the dangling amino groups and the surface silanols [35].

The SF silica presents contact angles of *ca.* 100°, a similar value to the 98° found by Song and coworkers [38] for silica surfaces modified with methyl groups. TMCS-functionalized surfaces often have contact angles as high as 150° [39]. Rao et al. found contact angles between 115 and 136° to surfaces functionalized with different amounts of di-methyl-chloro-silane [40]. This higher contact angle of the SF films with respect to the NF and OSF samples is due to the much higher hydrophobic character of the −Si−(CH$_3$)$_3$ groups relative to amino or silanol surface functions at any pH. The contact angle measured for the TMCS-functionalized sample is however significantly lower than some of the values presented in literature [39]. This is probably due to the presence of amino groups located close to the surface that could confer a partial hydrophilic character.

EEP measurements reveal that both OSF and SF films present very similar pore volumes and almost the same values of pore and neck sizes, and thickness (Fig. 2b), as could be expected, since both materials were synthesized employing the same method and using the same structuring agent. Pore and neck sizes presented on Table 1 were ~3 nm and ~2.5 nm, respectively. The minor differences observed between the pore diameter obtained by ellipso-porosimetry and electron microscopy can be explained considering the uncertainty of the diameter measurement directly of the micrograph in the latter technique. It can be concluded that the amino functionalization process in both approaches (SF and OSF) leads practically to the same pore modification.

XPS and EDS analysis were performed with the aim of comparing the N concentrations (from the APTES) present on the outer surface of the material and on the inner surface of the mesopores, and reported in Table 1. EDS spectra of SF and OSF were measured to sense the presence of N within the whole material due to its higher penetration in the sample (ca. 700 nm using an approximation by Potts [41], versus the ~200 nm film thickness). Although EDS is not a fully quantitative measurement, the N content of the samples was measured in normalized acquisition conditions, on films with the same thickness, which leads to reproducible results [42]. A thorough examination along the whole samples gave homogeneous and consistent results of the N composition within 5% uncertainty.

The penetration depth of XPS in mesoporous silica thin films is in the order of ~9 nm (electron attenuation length ~3 nm); thus, XPS probes the film surface, pore openings, and film walls up to a thickness of approximately the first two pore layers, as shown in previous work [35]. Both the selectively functionalized (SF) and the one-step functionalized (OSF) mesoporous silica samples were analyzed by the two techniques. In order to make a quantitative comparison between both kinds of films, it is necessary to perform the analysis on samples with similar density (hence, porosity), in order to ensure that the spatial region probed by XPS is the same. This is the case of the analyzed SF and OSF samples, in which pore volume, neck diameter and pore diameter are very similar (see Table 1). XP spectra (Fig. 3a) for both samples show a broad signal that can be fitted with two major components, according to previously reported values for APTES-functionalized mesoporous silica thin films [35]. The low binding energy component centered at 398.5 eV is assigned to the −NH$_2$ moiety, whereas the high binding energy peak at 401.8 eV is due to the protonated amine −NH$_3^+$,

In the case of the SF spectrum, the presence of the band at 398.5 eV could be observed. On the other hand, the OSF spectrum can be clearly deconvoluted in two peaks correspondent to the −NH$_2$ and −NH$_3^+$ groups (Fig. 3b). Using the rationale developed in previous works in APTES-functionalized mesoporous thin films [35,36], the ratio of unprotonated to protonated species is approximately ~0.1, indicating that the amine groups are approximately 90% protonated, which is consistent with the pH~5 at which the samples were exposed [35]. The presence of N in the XPS analysis of the SF sample, may be due to the presence of −NH$_3^+$ (or−NH$_2$) groups near the outer surface; however the XP spectra clearly shows that the amount of N present on the SF sample is significantly lower than the amount present in the OSF.

From Table 1 it can be clearly seen that in the EDS analysis, the ratio between the area of the nitrogen peaks for samples OSF/SF is practically 1 within the experimental uncertainty, whereas XPS analysis shows an OSF/SF relationship of 4.3. This decrease in the N contents in the SF samples is consistent with a selective surface modification with organic functions that do not contain amino groups. As mentioned above, EDS analyzes the entire volume of the material. Since the top surface of the films is very small relative to the inner surface of the mesoporous material, it is expected that EDS analysis will virtually not show differences between the two types of synthesized materials. In XPS analysis, in contrast, the 9 nm

Table 1
EDS/XPS comparative analysis, water contact angles measurements, and porosity, pore and neck sizes determined through EEP.

Sample	EDS/ Atomic %	XPS/ N counts	Contact angle/ °	Pore volume/ %	Pore diam./ nm	Neck diam./ nm
NFS	–	–	33	–	–	–
SF	18 ± 1	713.0	103	22	3.0	2.5
OSF	19 ± 1	3073.0	70	25	2.8	2.3
OSF/SF	1.05	4.3	–	–	–	–

penetration allows analyzing primarily the outer surface of the material. The outer surface of the material in which the conventional functionalization has been performed presents a significantly higher N content than the outer surface of the material which was selectively functionalized, strongly suggesting that a selective functionalization process took place that enables a spatially adjustable functional material.

When analyzed together, the evidence gathered by the EDS, XPS and contact angle experiments lead to propose that the SF samples are covered by trimethylsilane functions on their top surface, and amino functions in the pore surface below. A very minor $-NH_2$ fraction added during the second step of functionalization to the SF samples can be located either in the pores closer to the surface, or even occupying a minor fraction of the top surface layer sites. The presence of these more hydrophilic functions can explain the observed value of the contact angles, which is significantly lower than a fully hydrophobic trimethylated surface. Our experiments cannot assess the in-depth distribution of both functions along film thickness, and the existence of trimethyl groups in the top pore layers of SF samples due to partial template loss along the first functionalization process cannot be ruled out. However, the presented results clearly show the different distributions of the amino functions in both film processing processes, and that the SF method presented here effectively leads to a selective positioning of the trimethyl function near the top film surface, leaving the amino groups at the pore interior.

4. Conclusions

In this work, a simple and reproducible three-step method for the selective functionalization of the inner/outer surface of a mesoporous silica thin film is presented. The external surface functionalization of the mesoporous film (i.e., top film surface) was achieved by exposing the films to vapors of trimethylchlorosilane, followed by template extraction and inner pore functionalization with amino groups using a common post grafting technique with APTES.

The combination of contact angle measurements, XPS and EDS allowed to determine that the amount of propylamino functions located in the upper surface by this procedure was significantly different from the one obtained through the usually employed post-grafting technique. The amount of $-NH_2$ functions within the intra pore surface was almost the same for both functionalization routes. Thus, it could be concluded that amino and trymethyl silane functions can be distributed selectively on the external film surface or the mesopore surface of the thin film.

The choice of functionalizing agents for the three-step process implies selecting a volatile and reactive molecule to modify the external surface. These two aspects are important in order to optimize transport in the vapor phase, and minimize penetration in the inner pore surface. In this particular work, TMCS is a suitable molecule; in addition, trimethyl and amino functions present significantly different behavior regarding philicity, which facilitates the determination of the functional groups location in the pore network.

In contrast to the methods previously presented in literature, the method presented here is simple, does not require high working temperatures nor aggressive media, and can be carried out using a wide variety of volatile silanes as functionalizing agents. This allows particularly the selective functionalization of thin films, which tend to be less stable and prone to fast diffusion, but can also be extended to mesoporous particles.

This procedure can be easily adapted to a wide variety of volatile silane-based molecules, permitting to develop a general pathway to modify mesoporous thin films with different groups in the inner and outer surface of the mesoporous oxide. An intelligent surface control can be achieved using the method presented here, allowing the use of different anchor groups ($-R-SH$, $-R-NH_2$, $-R-H_2PO_3$, etc.) selectively located in the mesoporous material for different functions. This opens up a new pathway to the synthesis of multifunctional mesoporous thin films that can be applied as molecular filters with molecular switches, displaying control barriers simultaneously responsive to different stimuli [17,24].

References

[1] G.J.A.A. Soler-Illia, P.C. Angelomé, M.C. Fuertes, A. Calvo, A. Wolosiuk, A. Zelcer, M.G. Bellino, E.D. Martinez, J. Sol–Gel Sci. Technol. 57 (2011) 299–312.
[2] P. Innocenzi, L. Malfatti, Chem. Soc. Rev. 42 (2013) 4198–4216.
[3] C. Sanchez, C. Boissière, D. Grosso, C. Laberty, L. Nicole, Chem. Mater. 20 (2008) 682–737.
[4] G.J.A.A. Soler-Illia, P. Innocenzi, Chem. Eur. J. 12 (2006) 4478–4494.
[5] F. Hoffmann, M. Cornelius, J. Morell, M. Fröba, Angew. Chem. Int. Ed. 45 (20) (2006) 3216–3251.
[6] G.J.A.A. Soler-Illia, O. Azzaroni, Chem. Soc. Rev. 40 (2011) 1107–1150.
[7] F. Goettmann, C. Sanchez, J. Mater. Chem. 17 (2007) 24–30.
[8] R.A. Schoonheydt, B.M. Weckhuysen, Phys. Chem. Chem. Phys. 11 (2009) 2794–2798.
[9] G.J.A.A. Soler-Illia, C. Sanchez, B. Lebeau, J. Patarin, Chem. Rev. 102 (2002) 4093–4138.
[10] P. Valle-Vigón, M. Sevilla, A.B. Fuertes, Mater. Chem. Phys. 139 (2013) 281–289.
[11] H. Yuan, J.Q. Xu, L. Xie, Mater. Chem. Phys. 129 (2011) 1195–1200.
[12] J.S. Beck, J.C. Vartuli, W.J. Roth, M.E. Leonowitcz, C.T. Kresge, K.D. Schmitt, C.T.W. Chu, D.H. Olson, E.W. Sheppard, S.B. McMullen, J.B. Higgins, J.L. Schlenker, J. Am. Chem. Soc. 114 (1992) 10834–10843.
[13] A. Ciferri, Supramolecular Polymers Ed., CRC Press, Boca Raton, FL, 2005.
[14] I.W. Hamley, Introduction to Soft Matter: Synthetic and Biological Self-assembling Materials, John Wiley & Sons, West Sussex, 2007.
[15] D. Rodríguez-Fernández, J. Pérez-Juste, I. Pastoriza-Santos, L.M. Liz-Marzán, Chem. Open 1 (2012) 90–95.
[16] S. Jiang, M.J. Schultz, Q. Chen, J.S. Moore, S. Granick, Langmuir 24 (2008) 10073–10077.
[17] S. Alberti, G.J.A.A. Soler-Illia, O. Azzaroni, Chem. Commun. 51 (2015) 6050–6075.
[18] F. de Juan, E. Ruiz-Hitzky, Adv. Mater. 12 (6) (2000) 430–432.
[19] M.H. Lim, A. Stein, Chem. Mater. 11 (1999) 3285–3295.

[20] V. Cauda, A. Schlossbauer, J. Kecht, A. Zurner, T. Bein, J. Am. Chem. Soc. 131 (2009) 11361—11370.
[21] J. Kecht, A. Schlossbauer, T. Bein, Chem. Mater. 20 (2008) 7207—7214.
[22] K.A. Kilian, T. Böcking, K. Gaus, J.J. Gooding, Angew. Chem. Int. Ed. 47 (2008) 2697—2699.
[23] W. Xu, J. Rytkönen, S. Rönkkö, T. Nissinen, T. Kinnunen, M. Suvanto, A. Närvänen, V.P. Lehto, Chem. Mater. 26 (2014) 6734—6742.
[24] D. Brühwiler, Nanoscale 2 (2010) 887—892.
[25] D.S. Shephard, W. Zhou, T. Maschmeyer, J.M. Matters, C.L. Roper, S. Parsons, B.F.G. Johnson, M.J. Duer, Angew. Chem. Int. Ed. 37 (1998) 2719—2723.
[26] C. Argyo, V. Weiss, C. Bräuchle, T. Bein, Chem. Mater. 26 (2014) 435—451.
[27] M.J. Juan-Díaz, M. Martínez-Ibáñez, M. Hernández-Escolano, L. Cabedo, R. Izquierdo, J. Suay, M. Gurruchaga, I. Goñi, Progr. Org. Coat. 77 (2014) 1799—1806.
[28] D.R. Dunphy, S. Singer, A.W. Cook, B. Smarsly, D.A. Doshi, C.J. Brinker, Langmuir 19 (2003) 10403—10408.
[29] A. Grycová, G. Kejmarová, J. Matouek, Ceram—Silikáty 46 (2002) 49—51.
[30] J.D. Bass, D. Grosso, C. Boissiere, E. Belamie, T. Coradin, C. Sanchez, Chem. Mater. 19 (2007) 4349—4356.
[31] M.G. Bellino, A.E. Regazzoni, G.J.A.A. Soler-Illia, ACS Appl. Mater. Interfaces 2 (2010) 360—365.
[32] P.C. Angelomé, M.C. Fuertes, G.J.A.A. Soler-Illia, Adv. Mater. 18 (2006) 2397—2402.
[33] C. Boissiere, D. Grosso, S. Lepoutre, L. Nicole, A.B. Bruneau, C. Sanchez, Langmuir 21 (26) (2005) 12362—12371.
[34] B. Dittert, F. Stenzel, G. Ziegler, J. Non-Cryst. Solids 352 (2006) 5437—5443.
[35] A. Calvo, P.C. Angelomé, V.M. Sánchez, D.A. Scherlis, F.J. Williams, G.J.A.A. Soler-Illia, Chem. Mater. 20 (2008) 4661—4668.
[36] A. Calvo, M. Joselevich, G.J.A.A. Soler-Illia, F. Williams, J. Microporous Mesoporous Mater. 121 (2009) 67—72.
[37] R. Rosario, D. Gust, M. Hayes, F. Jahnke, J. Springer, A.A. Garcia, Langmuir 18 (2002) 8062—8069.
[38] J. Yang, J. Chen, J.H. Song, J. Vib. Spectrosc. 50 (2009) 178—184.
[39] S.D. Bhagat, Y.-H. Kim, K.-H. Suh, Y.-S. Ahn, J.-G. Yeo, J.-H. Han, Microporous Mesoporous Mater 112 (2008) 504—509.
[40] S.A. Mahadik, M.S. Kavale, S.K. Mukherjee, A.V. Rao, Appl. Surf. Sci. 257 (2010) 333—339.
[41] P.J. Potts, A Handbook of Silicate Rock Analysis, Chapman and Hall, New York, 1987, p. 336.
[42] T. Conard, K. Arstila, A. Hantschel, A. Franquet, W. Vandervorst, E. Vecchio, S. Burgess, F. Bauer, Mater. Res. Soc. Symp. Proc. 1184 (2009) 191—196.